JOURNAL OF NEUROTRAUMA
Volume 9, Number 4, 1992
Mary Ann Liebert, Inc., Publishers

# Biomechanical Aspects of a Fluid Percussion Model of Brain Injury

LAWRENCE E. THIBAULT,[1] DAVID F. MEANEY,[1] BRUCE J. ANDERSON,[2] and ANTHONY MARMAROU[2]



## ABSTRACT

**The fluid percussion model is in widespread use for the study of brain injury. However, the tissue deformation characteristics of the model have not been determined. Studies have suggested that at high levels of fluid percussion, the fluid percussion model is primarily a model of brainstem injury. It was proposed that this occurs as a direct result of the volume influx to the cranial vault at the moment of impact. This study examines the biomechanical deformation produced by the fluid percussion model. The purpose of this investigation was to describe the regional strain distribution in brain tissue at the moment of impact and to determine the effect of volume efflux produced by the percussion device. A cat skull was sectioned parasagittally and filled with an optically transparent gel. A grid pattern was painted in the midsagittal plane and was used to record the surrogate brain tissue deformation in response to fluid percussion loading. Motion of the grid pattern at low and high levels of fluid percussion loading was recorded using a high-speed camera, and a series of photographs developed from the high-speed film were analyzed to determine the intracranial strain distribution at these loading levels. The results of these studies indicated that the maximum site of strain was located in the region of the lower brainstem and that deformations were negligible in other regions of the brain. These studies provide an explanation for the pathophysiologic results obtained in a parallel series of experiments from which it was concluded that high-level fluid percussion is predominantly a model of lower brainstem injury.**

## INTRODUCTION

EXPERIMENTAL STUDIES HAVE INDICATED that high-level fluid percussion in the cat is predominantly a model of brainstem injury (Shima and Marmarou, 1991). In this fluid percussion injury model, a fluid column was placed in intimate contact with the dura, and it was hypothesized that the rapid influx of saline introduced by the percussion device was responsible for the structural damage to the brainstem. Following the completion

[1]Department of Bioengineering, The University of Pennsylvania, Philadelphia, Pennsylvania.
[2]Richard Roland Reynolds Neurosurgery Research Laboratories, Division of Neurosurgery, Medical College of Virginia, Richmond, Virginia.

of these pathologic studies, a collaborative effort was initiated to study the biomechanics of high-level fluid percussion injury. Heretofore, the tissue response of the fluid percussion model had not been explored.

The objective of this investigation was to describe the regional strain distribution in brain tissue at the moment of impact and to determine the effect of volume influx produced by the percussion model. A second goal was to determine the degree, based on theoretical considerations, to which mechanical insult produced by the percussion model mimics the biomechanics of severe head injury produced by inertial models (Abel et al., 1978; Gennarelli et al., 1982). This report describes the application of physical models, or surrogates, of the skull–brain structure and their use in providing insight into the mechanisms of neural and neurovascular tissue injury. Previous experiments have demonstrated that these models can be used to estimate the magnitude, temporal nature, and topographic distribution of the deformation pattern experienced by brain tissue under various prescribed loading conditions (Thibault, 1982; Margulies, 1987; Margulies et al., 1990; Meaney and Thibault, 1990; Meaney, 1991). Until now, physical model simulations and analyses have been directed toward inertial loading (acceleration)-induced brain injury in the primate. This study represents a continuation of our physical modeling approach to understanding the mechanisms responsible for brain injuries witnessed in other animal models of brain injury. To our knowledge this is the first application of this technology to a fluid percussion model.



## MATERIALS AND METHODS

A fluid percussion device, calibrated at the Medical College of Virginia, was transported to the University of Pennsylvania laboratories for use in these experiments. After calibrating and testing the device for satisfactory operation, a physical model was constructed in a manner similar to the method described in previous modeling studies (Margulies, 1987; Meaney, 1991). An illustration of the completed model using a cat skull is shown in Figure 1. The skull was prepared by cutting a parasagittal plane 1.0 cm lateral to the midline to produce a full sagittal view of the cranial cavity containing the right hemisphere. To attach the model to the percussion device, a 10 mm diameter hole was drilled in the vertex of the skull along the sagittal midline. In addition, the oval foramen magnum was made circular (D = 1.0 cm) in order to insert a surrogate Lucite spinal column. This surrogate spinal column consisted of a transparent Lucite right circular cylinder

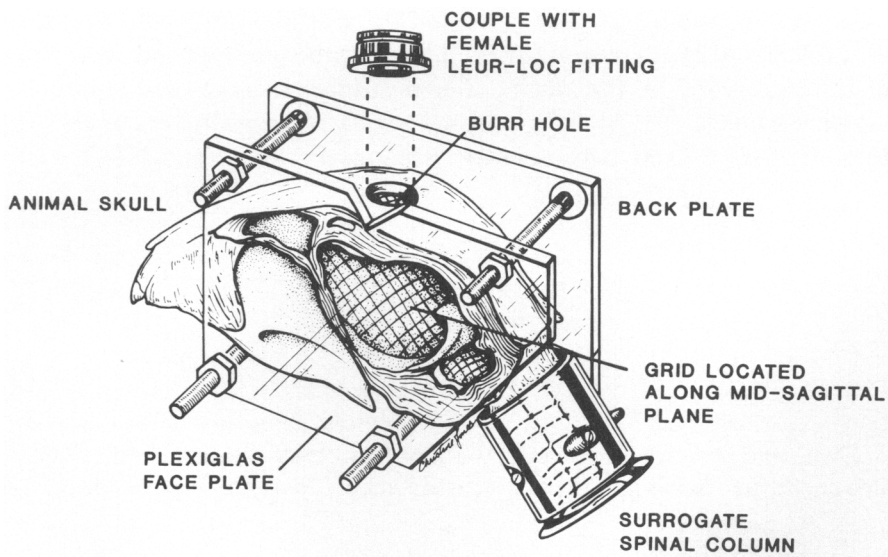


**FIG. 1.** Illustration of physical model used in this study. Fluid percussion insult was delivered through the opening located at the vertex of the cat skull. A painted grid pattern located in the midsagittal plane was used to measure the deformation of the surrogate brain material in response to fluid percussion loading.

(35 mm long, 1.0 cm ID) with a circular shoulder (5 mm thickness) for insertion into the machined foramen magnum. The interiors of both the skull and spinal column were painted white for photographic enhancement during high-speed filming.

After assembly of the skull and spinal column, Sylgard Medical Gel (Dow Corning, Midland, MI) was poured into the model until the gel level reached the sagittal midline. After proper curing of the gel (approximately 48 h), a black enamel grid (orthogonal, 2.5 mm spacing) was painted on the gel surface and allowed to dry thoroughly. At this point, a final layer of gel was poured over the grid plane, filling the remaining volume of the model. By casting the gel in this manner, a no-slip condition was created at the skull–gel interface. Once this final layer of gel had cured, the model was sealed by pressing two Lucite plates against front and back surface of the model. To ensure a tight seal between the front plate and the cut sagittal surface of the skull, a silicone rubber sealant (RTV 11, Dow Corning) was applied to the periphery of the skull before the assembly was tightened. When this gasket material had cured, deaerated water was injected into the space between the Lucite plate and the free surface of the gel, creating a pure slip boundary condition at this interface. The incompressibility of the water injected between the gel surface and the front Lucite plate minimized out of plane movement of the gel and grid mesh. The gel surface could move freely in a parasagittal plane to simulate the free brain motion occurring if a whole brain cast could be constructed. The assembled model was then coupled to the fluid percussion device, ready for testing.

The modulus of elasticity (E) of the silicone gel can be varied by changing the catalyst/polymer ratio of the gel components. In this study, the mixture of components (1:1) used produced a gel that displayed mechanical properties, as measured by static indentation, that were similar to identical indentation tests conducted on the exposed cortex in animal experiments ($E_{gel}$ = 0.680 psi, $E_{brain}$ = 0.417 psi) (Blum et al., 1985) and were within the range of values reported for brain tissue (E = 0.2–8.0 psi) (Fallenstein et al., 1969; Estes and McElhaney, 1970; Galford and McElhaney, 1970; Shuck and Advani, 1972).

Additionally, laboratory tests have indicated that the gel is elastic to stretch ratios of 3.0 or strains of 300%. Therefore, the material will return to its undeformed state when the load is removed. This characteristic allows one to reuse a physical model, so that multiple experimental loading conditions can be investigated using the same surrogate.

### *Injury Device*

The device used to deliver the mechanical insult to the model is described in more detail elsewhere (Sullivan et al., 1976). Briefly, it consists of a large Lucite cylinder (60 cm long, 4.5 cm ID) mounted horizontally to two support brackets, which in turn are attached to a steel base. One end of the cylinder is fitted with a piston equipped with O-rings to seal the piston end. The opposite end of the cylinder is connected to a 2 cm long tube containing a pressure transducer. Attached to this housing is an adapter that serves to couple the fluid-filled column to the skull model at the opening.

The mechanical load is produced by hitting the piston with a metal pendulum. Varying the pendulum release height changes the amplitude of the delivered pressure pulse. A photoelectric cell located near the pivot point of the pendulum initiates the recording of the pressure pulse on a digital storage oscilloscope. Pressure pulses were photographed using a Polaroid camera.

Deformation of the grid pattern at the plane of interest of the model during dynamic loading was recorded using a high-speed camera (HYCAM, Redlake Industries, Campbell, CA), which filmed the event at the rate of 6500 frames/sec. Every fourth frame of the high-speed film was enlarged and printed on 8 × 10 in photographic paper for digitizing purposes. Grid intersections were located and recorded for analysis using an HP 9836 computer and bit pad (Houston Instruments, Austin, TX). Figure 2 is a schematic representation of the experimental configuration of equipment and procedures.

### *Analysis*

The two descriptors used to measure the response of the surrogate brain tissue to fluid percussion loading were selected to reflect both the local deformation and regional displacement of the gel in the sagittal plane of the physical model. All descriptors were lagrangian, in that measurements were referenced to the original

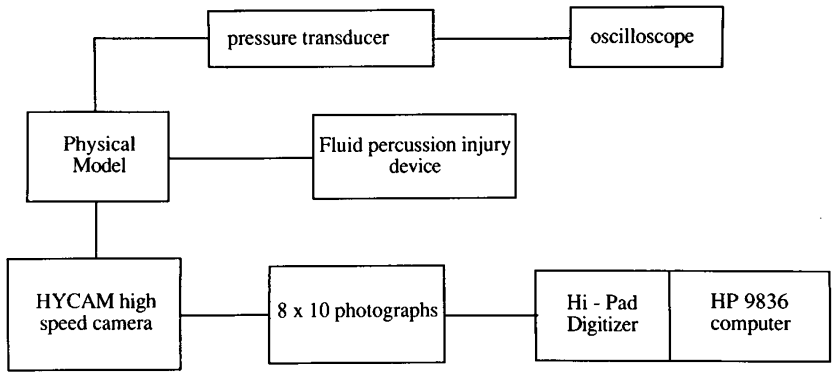


**FIG. 2.** Schematic of system used to record and measure surrogate tissue response from fluid percussion. High-speed filming (6500 frames/sec) recorded the grid deformation in the skull model. Grid deformation was tracked manually for the duration of the experiment using a digitizing tablet, and 8 × 10 still photographs were generated from the high-speed film (1 msec intervals). An HP 9836 computer was used to calculate appropriate mechanical field parameters.



undeformed grid pattern. Each measurement was taken directly from the photographs; no measures were inferred. Tissue deformation was defined using a stretch ratio ($\lambda$) as described by Equation (1) in the Appendix and was intended to provide a measure of the deformation experienced by the surrogate tissue in selected regions of the model. The nodal points selected for this analysis provided a direct measurement of the tissue deformation occurring in the cerebrum, lower brainstem, and cervical spinal cord. For measures in the lower brainstem and spinal cord, the orientation of the undeformed length ($l_0$) was chosen to coincide with the preferred direction of fibers residing in these areas. For consistency, the same orientation was used for the measurements in the cerebrum.

In addition, the regional displacement of material during the course of loading was described by the magnitude of the displacement vector ($\delta$) for any node point in the grid according to Equation (2) in the Appendix. Once again, three distinct anatomic regions (frontal lobe, supratentorial, and spinal cord) were analyzed. Using these measurements, the maximum local deformation for mild and severe fluid percussion loads and displacement time histories for various nodal locations were obtained.

## RESULTS

Once the photographic prints of the high-speed film were digitized, a computer-generated image was compiled for illustrative purposes (Fig. 3). Shown in Figure 3 are three images that represent separate times during the course of a high level of fluid percussion loading ($P_{peak}$ = 3.5 atm). At time equals zero, the grid is in the undeformed state, whereas at time equals 16 msec, the deformation pattern is at its maximum deformed state. The third image represents the state of deformation at time equals 30 msec and corresponds to that time when the load has returned to approximately zero. Note the hemispherical bulge that appears at the distal end of the surrogate spinal column in the second image. The volume of this deformed element represents the amount of material that was transiently extruded from the model at the time of maximum load. Herniation of material appears in response to the rise in pressure within the cranial vault. Since the gel, like brain tissue, is nearly incompressible, the pressure causes extrusion through the foramen magnum. On removal of this pressure, the gel material returns to the cranial vault. The absence of significant permanent herniation in this physical model is similar to the companion series of animal experiments, where no permanent lower brainstem extrusion was observed when removing the brain from the cranial vault.

Figure 4 shows the measured pressure for the high-level fluid percussion experiment and the calculated volume extrusion from the spinal column, assuming a hemispherical shape. Both are plotted as a function of time. The peak pressure recorded was 3.5 atm, and the maximum volume extruded from the model equaled

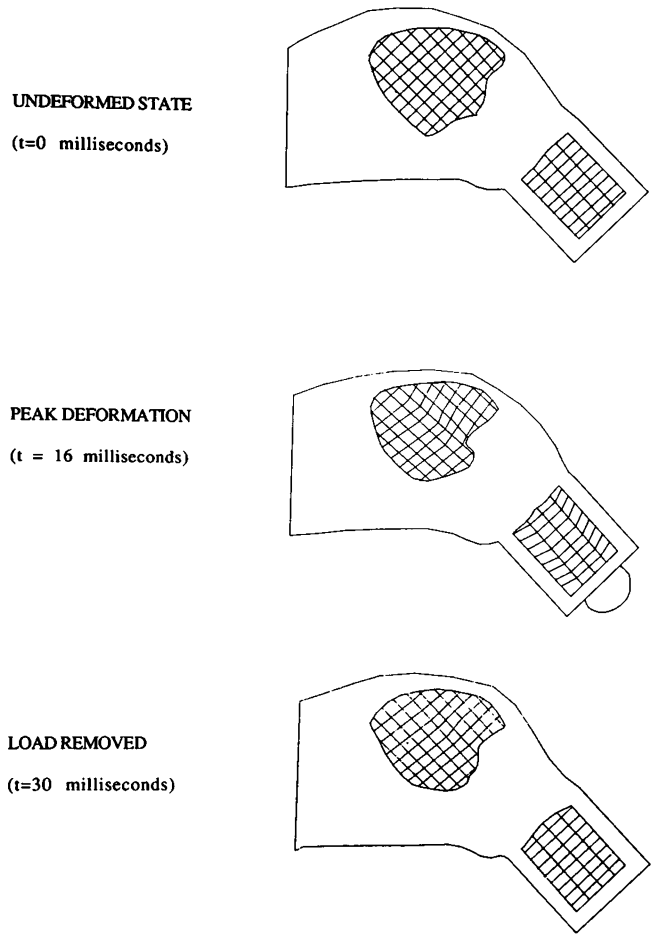


**FIG. 3.** Digitized reconstructed images of the model response to high-level fluid percussion (> 3.0 atm) loading. Note the volume of surrogate brain material extruded through the distal end of the spinal column at peak deformation (t = 16 msec).



0.7 ml. The phase differences between the percussion pulse and the extruded material volume are a function of the inertial lag of the gel during loading and an elastic overshoot following removal of the load. From these data, the pressure–volume index (PVI) occurring dynamically was calculated. The dynamic PVI should be significantly lower than the value for a static experiment. These results are discussed further in the next section.

Experiments were conducted at both the high and low levels of percussion. Figure 5A depicts the displacement of three nodal locations within the field during a low-level loading condition. The nodes represent frontal lobe, supratentorial, and spinal cord equivalent locations. Maximum displacement occurs in the spinal column and reaches a value of 2 mm, whereas the displacements within the surrogate brain (frontal lobe, supratentorial nodes) are approximately equal at 1 mm. The tissue deformation may be described as the difference in displacement between two nodal locations. One would expect in this instance to observe little or no strain between the supratentorial nodes but to find that the material in the region of the brainstem was undergoing stretch as a result of the difference in displacement between the supratentorial node and the spinal column node.

This portrait of differential displacement becomes much more noticeable when the experiment is conducted at the high level of fluid percussion. An example of the high-level loading condition is shown in Figure 5B. Again, the difference in nodal displacements within the brain are modest when comparing the frontal lobe

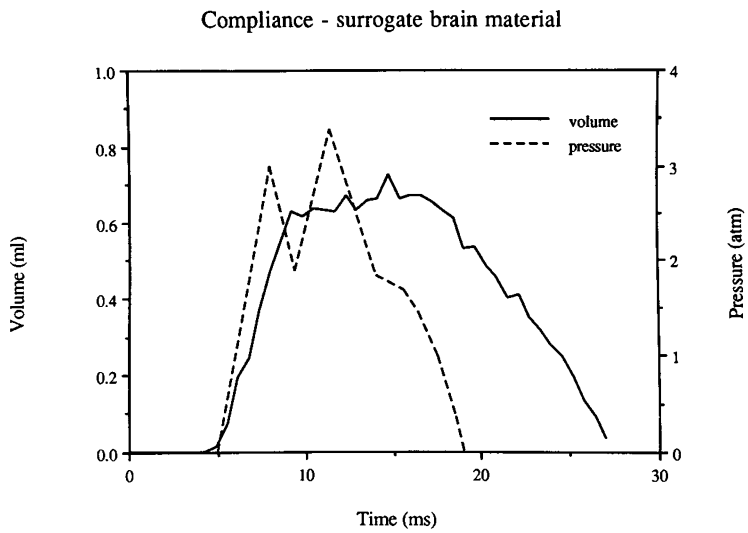


**FIG. 4.** Graph of pressure pulse insult and volume extrusion of surrogate material for high-level fluid percussion. The phase differences between the percussion pulse and the extruded material volume are due to the inertial lag of the material during loading and the elastic overshoot following removal of load.

region with the supratentorial location. However, the displacement in the spinal column of 5 mm was roughly double that in the surrogate brain. A calculation of stretch ratio using these nodal locations will serve to quantitate the apparent differences.

Figure 6A shows the strain ($\epsilon$) in the three regions described previously. The relationship between the stretch ratio ($\lambda$) and the strain ($\epsilon$) was defined as

$$\epsilon = \lambda - 1$$

The maximum strain was focused in the region of the brainstem, and for this low-level loading condition, the magnitude was 0.02, or 2% elongation of those tissue elements in the region. This level of fluid percussion reportedly produces a mild injury (Shima and Marmarou, 1991).

Figure 6B depicts the maximum strain under conditions of high-level fluid percussion. In contrast to the previous loading level, the peak magnitude of the elongating strain was approximately 0.11, or 11%. This level of tissue deformation has been shown to produce electrophysiologic changes in the isolated giant squid axon (Galbraith, 1988). Note, however, that the deformation is maximum in the brainstem and is much lower in the other regions of the model. This description of the topographic distribution of the deformations associated with high-level fluid percussion indicates that the primary site of injury is highly localized to the lower brainstem. This is in contrast to the inertial loading models, which have produced the largest deformations in the structures of the deep white matter of the brain (Gennarelli et al., 1982).

## DISCUSSION

Several forms of fluid percussion devices have evolved through the last two decades. The Sullivan device (Sullivan et al., 1976), developed for use in cats, was based on the intracranial volume loading device developed by Lindgren and Rinder (1969). Both of these devices have been shown by many investigators to produce graded pathophysiologic and morphologic changes that were correlated to the magnitude of the pressure pulse at the fluid-filled chamber of impact. However, in these models, the amount of fluid introduced into the cranial vault or the duration of the associated mechanical load could not be controlled. Stalhammer et al. (1987) modified the original design to allow precise control of the fluid volume introduced

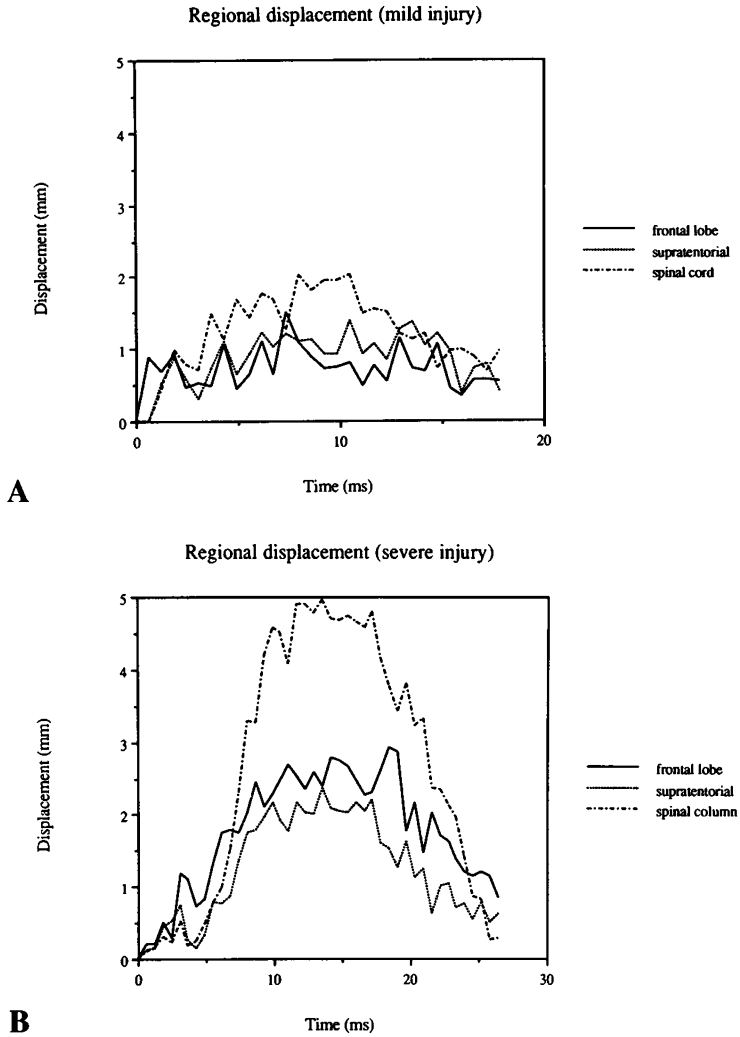


**FIG. 5.** Calculated displacement of grid elements located in the frontal lobe, supratentorial region, and spinal column area in response to low-level **(A)** and high-level **(B)** fluid percussion loading. Note the similar displacements of the frontal lobe and supratentorial locations and the larger displacement in the spinal cord region.



intracranially. These investigators concentrated their efforts on characterizing the volume loading, pressure peaks, and impulses associated with different settings of the device. However, a biomechanical analysis of the tissue response to such loading conditions was not undertaken.

Similarly, Dixon et al. (1988) modified the original Sullivan model for application to the rat and improved the fluid percussion technique by providing independent variation of the fluid pulse parameters. In these studies, cineradiographic images of the fluid on impact showed that the intracranial fluid movement was characterized by rapid radial movement within the epidural space. Rather than a focal insult to the exposed dura mater membrane, the fluid percussion pulse was found to spread diffusely across the superior brain surface. However, as in previous biomechanical analyses of fluid percussion, tissue deformation in response to these loading conditions was not studied.

Our study was designed to investigate, using biomechanical modeling techniques, the nature of the structural deformation associated with fluid percussion injury. Using these methods, we investigated the variation in the mechanical field parameters (displacement and strain) as a function of the experimental

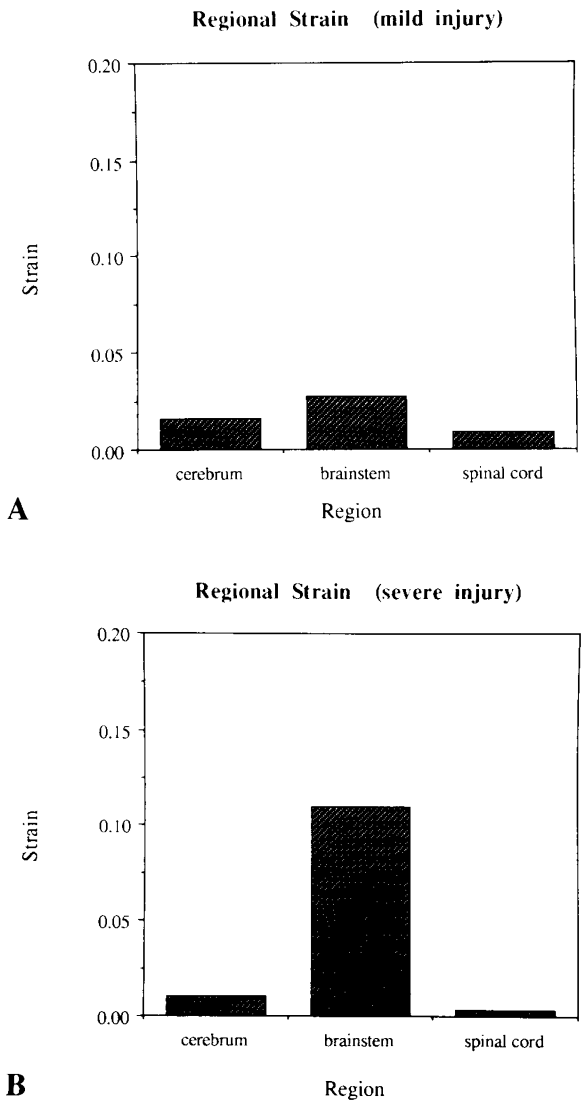


**FIG. 6.** Calculated regional strain ($\epsilon$) of the surrogate brain tissue as a result of low-level **(A)** and high-level **(B)** fluid percussion loading. For low-level insult, maximum strain was located in the lower brainstem region and was approximately 2%. For high-level insult, maximum strain was again located in the lower brainstem region and was approximately 11%. This level and rate of strain have been shown to cause electrophysiologic changes in the isolated squid giant axon (Galbraith, 1988).

loading conditions defined by a fluid percussion model for brain injury. Under the conditions of high-level fluid percussion, we observed that the strain field in the physical model is nonuniform and that the site of maximum strain is localized to the region of the lower brainstem.

Several methodologic considerations were taken into account when conducting the physical modeling study. First, the surrogate brain material was selected to provide a reasonable simulation of the actual brain material. To this end, the measured elastic modulus of the silicone gel material (E = 0.680 psi) falls within the range (E = 0.2–8.0 psi) reported for brain tissue. Second, the model did not attempt to simulate the flow of cerebrospinal fluid and blood from the intracranial cavity occurring from the mechanical insult. At present, the precise amount of cerebrospinal fluid and blood exiting the intracranial space during fluid percussion is unknown. However, the size of various foramina and blood vessels capable of transporting these fluids is much smaller than that of the foramen magnum, the primary conduit for tissue herniation, and the resistance

for cerebrospinal fluid and blood exudation would appear to be much higher than that for brain. The closed physical model configuration presented in this study is an approximation of this high resistance to cerebrospinal fluid and blood leakage. Third, the stretch ratio measurement was intended to provide an indication of the deformation of elements residing within different regions of the surrogate. The central finding of this report, the maximization of strain in the lower brainstem region during high-level fluid percussion, can be augmented by presenting a more refined depiction of the estimated strain and displacement fields occurring in the midsagittal plane during impact. As an example, one can compare the lesion patterns produced in the hemispheres to the spatial distribution of strain appearing in this region. Special attention can be placed on the area surrounding the percussion site, where a number of lesions have been found.

The calculated values for the strain are in excess of 10%, which suggests that the herniation of brain tissue through the foramen magnum will produce a stretch of the axons in the brainstem to a level that results in functional failure. Further, this degree of deformation may result in ultrastructural damage with residual deficit (Thibault et al., 1990). These observations are consistent with the findings discussed in previous physiologic study of the fluid percussion technique and reinforces the notion that high-level fluid percussion loading will produce a prominent lower brainstem injury. Although this study was confined to the central mode injury where percussion occurs directly on the vertex, the volume extrusion would be similar for lateral impact. The dynamic rise in intracranial pressure caused by the fluid percussion technique, which in turn causes extrusion of material through the foramen magnum, should be relatively independent of the loading site. Observations from the physiologic study cited earlier support this hypothesis, since lateral mode fluid percussion used in the pathophysiologic investigation produced predominantly lower brainstem injury.

Although the central and lateral mode fluid percussion models will produce similar lower brainstem injuries, a distinguishable lesion pattern should appear in the hemispheres. As indicated by Dixon et al. (1988), positioning the craniotomy at the vertex of the ferret skull will allow the percussion fluid to diffuse fairly symmetrically into the intracranial space, deforming the brain approximately equally in both hemispheres. In contrast, lateral mode percussion will preferentially direct the insult over the parasagittal cortex and cause the brain to deform asymmetrically, with the structures in the ipsilateral hemisphere experiencing a larger deformation than corresponding contralateral structures. This asymmetric deformation pattern may serve to explain the primarily ipsilateral hemisphere injuries reported by McIntosh et al. (1989) for a lateral fluid percussion model. It is worthwhile to note, though, that high levels of injury in this model (P = 3.0–3.6 atm) produced bilateral petechial hemorrhages in the brainstem similar to those observed in earlier vertex fluid percussion studies. Thus, repositioning the craniotomy did produce a different injury response in the hemispheres but did not eliminate the lower brainstem injury at high levels of fluid percussion.

In addition to correlating the deformation pattern of the surrogate brain material with the pathophysiologic findings, the physical model studies permit one to estimate the pressure–volume index (PVI) (Marmarou et al., 1978) for dynamic loading and the effective inertial loading condition that would produce an equivalent degree of tissue deformation. In the former case, the PVI is defined as

$$PVI \equiv \Delta V/\ln(p_{max}/p)$$

In these experiments, V and P are the instantaneous values of extruded volume and dynamic pressure, respectively. The PVI of the adult cat obtained by conventional bolus measurement is approximately 1 ml (Marmarou et al., 1978). For the physical model used in this study, a series of static hydrostatic pressure were used to determine a static PVI value for the model of milliliters. Conversely, under dynamic conditions, the calculated value of the PVI for the high-level fluid percussion study is 0.246 ml ($R^2 = 0.89$), which is approximately four times as stiff as the value for the static experiment. This increase in stiffness is related to the viscoelastic nature of the material where the response of the surrogate depends on the rate at which the load is applied. This would also be the case for brain tissue if the PVI was measured dynamically. Such a change in the material stiffness can be reproduced by studying a simple mechanical model of brain tissue. Using the reported values for the mechanical properties of brain tissue (shear modulus of 2 psi and a kinematic viscosity of 350 poise), the response of a Kelvin solid to the dynamic percussion loading yields an equivalent PVI of approximately 0.25 ml.

Finally, it is interesting to speculate the degree to which the lower brainstem deformation of either high-level lateral or central mode fluid percussion simulates the deformation produced by a pure inertial load.

A pure inertial load (translational acceleration) of the head can result in a dynamic pressure gradient within the cranial vault. The magnitude and gradient of this pressure within the tissue can be approximated for any given condition of inertial loading (Hayashi, 1969). Conversely, for a measured dynamic pressure of 3 atm at the foramen magnum, the equivalent inertial load would be in the inferior–superior direction, or equivalent to an impact of constant duration equal to approximately 15 msec. With this concept, the level of lower brainstem injury produced by high-level fluid percussion would be roughly equivalent to the level of injury produced by a translational acceleration of the head, along the superior–inferior axis, of approximately 2160 g. This loading would cause herniation of intracranial contents through the foramen magnum but would not include the damage that occurs to the cortex as a result of direct impact. However, experiments in both the rat and the cat show that cortical contusion at these injury levels is not a consistent feature of the percussion model. Further, this model of brain injury would not replicate the conditions of coronal plane rotational acceleration used to produce diffuse axonal injury in the subhuman primate (Gennarelli et al., 1982). The translational acceleration analog of fluid percussion will produce deformation patterns quite distinct from the strain patterns associated with the angular acceleration model. In the latter case, the measurable deformation occurs in the corpus callosum and the deep white matter of the brain. In the former case, the pressure appearing at the foramen magnum causes exudation of brain material and a localization of strain in the lower brainstem.

An alternative to the fluid percussion model has been proposed by Lighthall (1988). This model uses a rigid indentor to deliver a controlled cortical impact to the exposed dura of the ferret. Varying the velocity and penetration depth of the indentor yielded a spectrum of injuries ranging from mild dysfunction to death. The methodology outlined in this study, used to investigate inertial loading phenomena and now to study fluid percussion, can be applied also to this cortical impact model to study surrogate brain tissue deformation of this model.

In summary, this report illustrates that physical models can be used to evaluate the appropriateness of various animal models of brain injury by defining the regions of tissue damage and relating the magnitude of the strain in these equivalent anatomic locations in which the simulation is intended to replicate. When these methods were applied to fluid percussion injury, it was found that the region of maximum strain was focused in the brainstem. These observations are consistent with the pathophysiologic studies described in a previous study and provide a biomechanical explanation for the lower brainstem damage observed. This damage can be reduced by lowering the impact levels to less than 3.0 atm.



## ACKNOWLEDGMENTS

This work was supported in part by NIH grants NS-12587 and 5RO1NS19235-03, and CDC grant R49 CCR304684.

## REFERENCES

ABEL, J., GENNARELLI, T., and SEGAWA, H. (1978). Incidence and severity of cerebral concussion in the rhesus monkey following sagittal plane acceleration. Proc. 22nd Stapp Car Crash Conf. **22,** 33–53.

BLUM, R., THIBAULT, L., and GENNARELLI, T. (1985). In-vivo indentation of the cerebral cortex. Proc. 35th ACEMB, Chicago, IL, p. 86.

DIXON, C., LIGHTHALL, J.W., and ANDERSON, T.E. (1988). Physiologic, histopathologic, and cineradiographic characterization of a new fluid percussion model of experimental brain injury in the rat. J. Neurotrauma **5,** 91–104.

ESTES, M., and McELHANEY, J.H. (1970). Response of brain tissue to compressive loading. ASME paper no. 70-BHF-13, p. 13.

FALLENSTEIN, G., HULCE, V.D., and MELVIN, J.W. (1969). Dynamic mechanical properties of human brain tissue. J. Biomechanics **2,** 217–226.

GALBRAITH, J.A. (1988). *The Effects of Mechanical Loading on the Electrophysiology of the Giant Squid Axon.* Philadelphia: University of Pennsylvania.

GALFORD, J., and McELHANEY, J. (1970). A viscoelastic study of scalp, brain, and dura. J. Biomech. **3,** 211–221.

GENNARELLI, T., THIBAULT, L., ADAMS, J.H., GRAHAM, D.I., THOMPSON, C.J., and MARCININ, R.R. (1982). Diffuse axonal injury and prolonged coma in the primate. Ann. Neurol. **12,** 564–574.

HAYASHI, T. (1969). Study of intracranial pressure caused by head impact. J. Faculty Eng. Univ. Tokyo **(B)30,** 59–72.

LIGHTHALL, J. (1988). Controlled cortical impact: a new experimental brain injury model. J. Neurotrauma **5,** 1–15.

LINDGREN, S., and RINDER, L. (1969). Production and distribution of intracranial and intraspinal pressure changes at sudden extradural fluid volume input in rabbits. Acta Physiol. Scand. **76,** 340–351.

MARGULIES, S.S. (1987). *Biomechanics of Traumatic Coma in the Primate*. Philadelphia: University of Pennsylvania.

MARGULIES, S.S., THIBAULT, L., and GENNARELLI, T. (1990). Physical model simulations of brain injury in the primate. J. Biomech. **23,** 823–836.

MARMAROU, A., SHULMAN, K., and ROSENDE, R.M. (1978). A nonlinear analysis of the cerebrospinal fluid system and intracranial pressure dynamics. J. Neurosurg. **48,** 332–344.

McINTSOH, T.K., VINK, R., NOBLE, L., YAMAKAMI, I., FERNYAK, S., SOARES, H., and FADEN, A.L. (1989). Traumatic brain injury in the rat: characterization of a lateral fluid percussion model. Neuroscience **28,** 233–244.

MEANEY, D. (1991). *Biomechanics of Acute Subdural Hematoma in the Subhuman Primate and Man*. Philadelphia: University of Pennsylvania.

MEANEY, D.F., and THIBAULT, L.E. (1990). Physical model studies of cortical brain deformation in response to high strain rate inertial loading. Proc. 1990 IRCOBI Conf. Lyon, France, **11,** 215–224.

SHIMA, K., and MARMAROU, A. (1991). Evaluation of brainstem dysfunction following severe fluid-percussion injury to the cat. J. Neurosurg. **74,** 270–277.

SHUCK, L.Z., and ADVANI, S.H. (1972). Rheological response of human brain tissue in shear. J. Basic Eng. **94,** 905–911.

STALHAMMER, D., GALIANT, B.J., ALLEN, A.M., BECKER, D.P., and HAYES, R.L. (1987). A new model of concussive brain injury in the cat produced by extradural fluid volume loading: biomehcanical properties. Brain Injury **1,** 73–91.

SULLIVAN, H., MARTINEZ, J., BECKER, D.P., MILLER, J.D., GRIFFITH, R., and WIST, A.O. (1976). Fluid percussion of brain injury in the cat. J. Neurosurg. **45,** 520–534.

THIBAULT, L.E. (1982). Physical model experiments of the brain undergoing dynamic loading. In: *Advances in Bioengineering*. L.E. Thibault (ed.). New York, ASME, p. 172.

THIBAULT, L., GENNARELLI, T., MARGULIES, S.S., MARCUS, J., and EPPINGER, R. (1990). The strain-dependent pathophysiological consequences of inertial loading on the central nervous system. Proc. 1990 IRCOBI Conf., Lyon, France, **11,** 191–202.



## APPENDIX

The two descriptors used to measure the response of the surrogate brain tissue to fluid percussion loading were selected to reflect both the local deformation and regional displacement of the gel in the sagittal plane of the physical model. The stretch ratio ($\lambda$) was used to define the local surrogate tissue deformation and was expressed as

$$\lambda = l/l_0 \tag{1}$$

where deformed length of a line segment is l, and $l_0$ was defined as the undeformed length.

The regional displacement of material during the course of loading was described by the magnitude of the displacement vector ($\delta$) for any node point and was defined as

$$\delta = [(x - x_0)^2 + (y - y_0)^2]^{1/2} \tag{2}$$

where x,y = position of nodal point at time t, and $x_0$,$y_0$ = position of nodal point at time t = 0.

The maximum local deformation for mild and severe fluid percussion loads was calculated, and the displacement time histories for various nodal locations were measured.

Address reprint requests to:
*Lawrence E. Thibault, Sc.D.*
*University of Pennsylvania*
*Department of Bioengineering*
*Room 114 Hayden Hall*
*Philadelphia, PA 19104-6392*